Fermi National Accelerator Laboratory

FERMILAB-Pub-97/006-E
E687

Study of Charged Hadronic Five-body Decays of the D^+ and D_s^+ Mesons

P.L. Frabetti et al.
The E687 Collaboration

Fermi National Accelerator Laboratory
P.O. Box 500, Batavia, Illinois 60510

January 1997

Submitted to *Physics Letters B*

Operated by Universities Research Association Inc. under Contract No. DE-AC02-76CH03000 with the United States Department of Energy

Disclaimer

Distribution

Study of Charged Hadronic Five-body Decays of the D^+ and D_s^+ Mesons

E687 Collaboration

P. L. Frabetti

Dip. di Fisica dell'Università and INFN - Bologna, I-40126 Bologna, Italy

H. W. K. Cheung [a], J. P. Cumalat, C. Dallapiccola [b], J. F. Ginkel, W. E. Johns [c], M. S. Nehring [d]

University of Colorado, Boulder, CO 80309, USA

J. N. Butler, S. Cihangir, I. Gaines, P. H. Garbincius, L. Garren, S. A. Gourlay, D. J. Harding, P. Kasper, A. Kreymer, P. Lebrun, S. Shukla, M. Vittone

Fermilab, Batavia, IL 60510, USA

S. Bianco, F. L. Fabbri, S. Sarwar, A. Zallo

Laboratori Nazionali di Frascati dell'INFN, I-00044 Frascati, Italy

R. Culbertson [e], R. W. Gardner [f], R. Greene [g], J. Wiss

University of Illinois at Urbana-Champaign, Urbana, IL 61801, USA

G. Alimonti, G. Bellini, M. Boschini, D. Brambilla, B. Caccianiga, L. Cinquini [h], M. Di Corato, M. Giammarchi, M. Gullotta, P. Inzani, F. Leveraro, S. Malvezzi, D. Menasce, E. Meroni, L. Moroni, D. Pedrini, L. Perasso, F. Prelz, A. Sala, S. Sala, D. Torretta

Dip. di Fisica dell'Università and INFN - Milano, I-20133 Milan, Italy

D. Buchholz, D. Claes [i], B. Gobbi, B. O'Reilly [h]

Northwestern University, Evanston, IL 60208, USA

J. M. Bishop, N. M. Cason, C. J. Kennedy [j], G. N. Kim [k], T. F. Lin, D. L. Puseljic [j],
R. C. Ruchti, W. D. Shephard, J. A. Swiatek [l], Z. Y. Wu [m]
University of Notre Dame, Notre Dame, IN 46556, USA

V. Arena, G. Boca, C. Castoldi, G. Gianini, S. P. Ratti, C. Riccardi, L. Viola, P. Vitulo
Dip. di Fisica Nucleare e Teorica dell'Università and INFN - Pavia, I-27100 Pavia, Italy

A. Lopez, University of Puerto Rico at Mayaguez, Puerto Rico

G. P. Grim, V. S. Paolone [n], P. M. Yager, University of California-Davis, Davis, CA 95616, USA

J. R. Wilson University of South Carolina, Columbia, SC 29208, USA

P. D. Sheldon Vanderbilt University, Nashville, TN 37235, USA

F. Davenport University of North Carolina-Asheville, Asheville, NC 28804, USA

K. Danyo [o], T. Handler University of Tennessee, Knoxville, TN 37996, USA

B. G. Cheon [p], J. S. Kang, K. Y. Kim
Korea University, Seoul 136-701, Korea

Abstract

Charged hadronic five-body decays of D^+ and D_s^+ mesons have been studied in the E687 photoproduction experiment at Fermilab. We report the first compelling evidence of the decay mode $D^+, D_s^+ \to \pi^-\pi^-\pi^+\pi^+\pi^+$ and the measurements of the decays $D^+ \to K^-\pi^-\pi^+\pi^+\pi^+$, $D_s^+ \to K^-K^+\pi^-\pi^+\pi^+$ and $D_s^+ \to \phi\pi^-\pi^+\pi^+$. An analysis of the $D^+ \to K^-\pi^-\pi^+\pi^+\pi^+$ resonance structure is also presented.

The study of the hadronic decays of charm mesons has been proved to be a very productive and active field in recent years. While several experimental measurements are now available on five-body body decays [1] [2] [3], the theoretical predictions are limited mainly to two-body decay modes [4]. The hadronic processes are difficult to calculate because of gluon exchange among the quarks in the initial and final states. In addition the hadrons in the final state can rescatter into one another, these processes are referred as final-state interactions(FSI) [5].

Although D meson decays are dominated by two-body modes, it is worthwhile to complete the experimental picture of the charm meson decays with the study of the multi-body modes.

In this letter we continue (see for example reference [6]) our study on multi-body hadronic decay modes, by presenting results from D^+ and D_s^+ decays into five charged particles. We present the first compelling evidence of the decay mode $D^+(D_s^+) \rightarrow \pi^-\pi^-\pi^+\pi^+\pi^+$(throughout this paper the charge conjugate state is implied).

These modes may be produced as nonresonant final states or via multi-body intermediate resonant states. A study of the $D^+ \rightarrow K^-\pi^-\pi^+\pi^+\pi^+$ resonance structure, treated as an incoherent superposition of resonances, is also presented.

This analysis is based on data collected during the 1990-1991 fixed target run at Fermilab with the E687 spectrometer which is described in detail elsewhere [7]. A bremsstrahlung photon beam of mean energy approximately $200\,GeV$ impinges on a 4.4cm Be target; particles from the interaction are detected in a large aperture magnetic spectrometer with excellent vertex measurement, particle identification and calorimetric capabilities. Kaons and pions in the D meson final states are well separated in the momentum range $4.5 - 61\,GeV/c$ using three multicell Čerenkov counters. D^+ and D_s^+ primary (production) and secondary (decay) vertices are resolved by means of a high resolution vertex detector consisting of 12 microstrip planes. The resolution in the transverse plane is approximately $9\,\mu m$ in the target region.

The five-body D^+ (D_s^+) final states are selected using a *candidate driven vertex algorithm* [7]. A secondary vertex is formed from the five reconstructed tracks and the momentum vector of the D^+ (D_s^+) candidate is used as a seed to intersect the other tracks in the event to find the primary vertex. Once the production and decay vertices are determined, the distance ℓ between them and the relative error σ_ℓ are computed. Cuts on the ℓ/σ_ℓ ratio are applied to extract the D^+ (D_s^+) signals from the background. The topological configuration of the event is tested in four ways: the primary and secondary vertex confidence levels (a minimum value of 2% for the primary and secondary C.L. was required) and two measures of vertex isolation, a *no point-back isolation* and a *secondary vertex isolation.* The *no point-back isolation* cut required that the maximum confidence level for a candidate D^+ (D_s^+) daughter track to form a vertex with the tracks from the primary vertex was less than 20%. The *secondary vertex isolation* cut required that the maximum confidence level for another track to form a vertex with the D^+ (D_s^+) candidate be less than 1%. The four modes reported here are normalized to the two prominent decay modes of the D^+ and D_s^+: $D^+ \to K^-\pi^+\pi^+$ and $D_s^+ \to K^-K^+\pi^+$ *.

We turn next to a discussion of the additional analysis cuts we used to study the 3 basic decay topologies discussed in this paper, beginning with the five pion mode. The D^+ (D_s^+) $\to \pi^-\pi^-\pi^+\pi^+\pi^+$ decay mode is particularly difficult to detect because of the large combinatorial background. In order to suppress the large combinatoric background present in the five pion decay mode, we made the additional requirement that the secondary vertex lies downstream of our 4.4 cm. long Be target. Without this *out of target* cut the signals are barely visible. We believe that the source of this background is the secondary interaction of the particles(mostly pions) produced in non-charm primary vertices. Such a secondary vertex interaction, in fact, will have a significant detachment from the primary and thus mimic the topology of a *charm* decay. Hence our standard vertex cuts are inefficient in removing this type of background. In this analysis only the five track combinations

*We prefer to normalize to the inclusive $D_s^+ \to K^-K^+\pi^+$ decay mode rather than to the intermediate state resonant mode $D_s^+ \to \phi\pi^+$ because of the possibility of interference [8].

satisfying loose pion identification requirements (i.e. no pions are identified as either kaons or protons by the Čerenkov system) are kept. Finally we require the D^+, D_s^+ reconstructed momentum be greater than 25 GeV/c. We also imposed a series of cuts designed to remove backgrounds from misidentified charm decays and $D^\star$'s. In order to remove backgrounds from $D^{\star +} \to \pi^+ D^0$, $D^0 \to 4\pi$ we reject events with $\pi^-\pi^+\pi^-\pi^+$ invariant mass within 2σ from the nominal value of D^0 [9]. We also reject events which lie within 2σ of the D^+ mass when reconstructed as $K^-\pi^-\pi^+\pi^+\pi^+$.

Figure 1a shows the five pion invariant mass plot obtained for these candidates with primary secondary vertex detachment cut of $\ell \geq 8\sigma_\ell$. The 5π invariant mass distribution is fitted with a Gaussian for the D^+ signal, a second Gaussian for the D_s^+ signal and a 2^{nd} degree polynomial for the background. Because of the limited statistics in the fit procedure the D^+ and D_s^+ masses are fixed to the world average [9] and the widths to those predicted by our Monte Carlo. Possible contamination due to other charm hadron decays involving either an additional π^0 or charged pions outside the spectrometer acceptance would affect only the low mass region which is therefore excluded from the fit. A binned maximum likelihood fit gives 58 ± 10 $D^+ \to \pi^-\pi^-\pi^+\pi^+\pi^+$ and 37 ± 9 $D_s^+ \to \pi^-\pi^-\pi^+\pi^+\pi^+$ events.

In the $D^+ \to K^-\pi^-\pi^+\pi^+\pi^+$ analysis, the requirement that one track be identified as a potential kaon suffices to reduce background due to the secondary interactions, and therefore no *out of target* cut is applied. We use very loose Čerenkov cuts both for the kaons and pions. Kaon candidates are essentially required to have a Čerenkov response inconsistent with being an electron or pion. Pion candidates are required to have a Čerenkov response inconsistent with being positively identified as kaons or protons. The fraction of events falling into each particle identification class was reproduced by our Monte Carlo simulation. Suitable vertex cuts are then applied to reduce the combinatorial background. We required that the D^+ reconstructed momentum be greater than 25 GeV/c. In order to remove $D^{\star +} \to \pi^+ D^0$ background we discard the events with an invariant mass of the combination $K^-\pi^+\pi^-\pi^+$ within 2σ from the D^0. In order to remove misidentified five pion decays, we discard the events with an invariant mass of the combination $\pi^-\pi^-\pi^+\pi^+\pi^+$ within 2σ from the D^+. Figure 1b show the invariant mass plot for these candidates satisfying the additional detachment cut of $\ell \geq 8\sigma_\ell$. The $K^-\pi^-\pi^+\pi^+\pi^+$ invariant mass distribution is fitted with a Gaussian signal peak over a second degree polynomial background. A signal of 239 ± 21 $D^+ \to K^-\pi^-\pi^+\pi^+\pi^+$ events is determined by a binned maximum likelihood fit.

For the $D_s^+ \to K^-K^+\pi^-\pi^+\pi^+$ decay, the joint requirement of two kaons in the final state reduces the background and allows us to use the same (very loose) Čerenkov cuts of the $D^+ \to K^-\pi^-\pi^+\pi^+\pi^+$ analysis. No *out of target* cut was necessary and the primary vertex confidence level cut was reduced to 1%. In addition, as was the case in our published [6] study of the $D^0 \to K^-K^+\pi^-\pi^+$ final state, we dropped the *no point-back isolation* cut. Because the energy release, Q, is small for these decays, tracks emerge in the laboratory with small angles with respect to the D line of flight and therefore appear to originate from the primary vertex. Figure 1c shows the invariant mass plot for $K^-K^+\pi^-\pi^+\pi^+$ combinations satisfying the $\ell \geq 8\sigma_\ell$ detachment cut. A binned maximum likelihood fit using a Gaussian signal peak and a second degree polynomial background gives 75 ± 13 events. Again we constrain the D_s^+ mass and width in this low statistics fit. For this final state we have studied also the subresonant decay mode $D_s^+ \to \phi\pi^-\pi^+\pi^+$. In addition to the previous cuts we require that the invariant mass of the K^-K^+ combination be consistent with the ϕ mass, that is $1.011 < M_{K^-K^+} < 1.027$ to take into account the detector resolution. The resulting histogram is shown in Figure 1d. A binned maximum likelihood fit using a Gaussian signal peak and a second degree polynomial background gives 40 ± 8 events.

We measure the branching fractions of these modes relative to $D^+ \to K^-\pi^+\pi^+$ and $D_s^+ \to K^-K^+\pi^+$. To minimize systematic effects, the normalizing decay mode is selected using the same vertexing cuts of the considered mode and analogous Čerenkov identification requirements. Our final measurements have been tested by modifying each of the vertex cuts individually; the results were always consistent within the errors[†]. Table I compares the

---

[†]In the case of the $D_s^+ \to K^-K^+\pi^-\pi^+\pi^+$ decay mode a contribution, due to a residual dependence

branching ratios obtained using an efficiency[‡] corrected yield with previous measurements. In addition Table II compares our result for the branching ratio $\Gamma(\phi 3\pi)/\Gamma(\phi\pi)$ with previous measurements. Our result is lower than the previous determinations although the errors are large.

The systematic errors on these measurements reflect uncertainties in reconstruction efficiency, Čerenkov particle identification and hadronic absorption of secondaries in the target and spectrometer materials. We follow a procedure similar to our previous analysis of the four-body decays [6]. The estimates were obtained by splitting our data into disjoint samples depending on the $D^+(D_s^+)$ momentum and the different periods in which the data were collected. The *split sample* variance is then defined as the difference between the reported statistical variance and the scaled variance if the scaled variance exceeds the statistical variance. The evaluation of systematic effects related to different fit procedures is performed on the whole sample. The branching ratios are calculated varying the fit conditions[§] and the sample variance is used because the fit variants are all a priori likely. The *split sample* variance and the variance from the different fitting procedures are then added in quadrature to obtain the systematic error.

The reported measurements of the five-body decays of the $D^+(D_s^+)$ meson are inclusive measurements. We have additionally studied the resonance substructure in the decay $D^+ \rightarrow K^-\pi^-\pi^+\pi^+\pi^+$.

We use a simplified approach to fit the resonance substructure in the decay $D^+ \rightarrow K^-\pi^-\pi^+\pi^+\pi^+$ which assumes that the final state is the result of an incoherent superposition of decay modes containing the common lowest mass $(K^-\pi^+)$ and $(\pi^-\pi^+)$

---

from the vertex cuts, has been added to the systematic error.

[‡]The efficiency for $D^+ \rightarrow K^-\pi^-\pi^+\pi^+\pi^+$ was calculated assuming the final state is composed of a mixture of intermediate decay modes determined by our resonant analysis which follows.

[§]These include the background shape and the Gaussian parameters.

resonances plus a five-body nonresonant channel[**]: $\overline{K^{*0}}\pi^-\pi^+\pi^+$, $K^-\rho^0\pi^+\pi^+$, $\overline{K^{*0}}\rho^0\pi^+$ and $(K\pi\pi\pi\pi)_{NR}$.

We extract the acceptance corrected event yield into each decay mode using a weighting technique where each event is weighted according to the values taken by specific two-body submasses in the five-body final state similar to that used in reference [6]. The weights are obtained using information from separate Monte Carlo simulations for each of the 4 decay modes and the formalism of a linear fit. The acceptance corrected event yields may be determined through a χ^2 fit to the number of observed signal events found in each three-dimensional bin defined in terms of the three submasses:[††] $(K^-\pi^+)$, $(\pi^-\pi^+)$, and $(\pi^+\pi^+)$. In the absence of interference between the decay modes, the number of predicted signal events in each bin would be a linear transformation T of the fit parameters (which are the acceptance corrected event yields). Since the fit is linear the fit parameters can in turn be expressed as a linear transformation R of the observed bin populations. This R matrix, which multiplies a column vector of observed bin populations to produce a column vector of acceptance corrected yields for the decay modes, is constructed using the T matrix which is computed from Monte Carlo.

An equivalent procedure, which we apply here, creates separate $K^-\pi^-\pi^+\pi^+\pi^+$ invariant mass histograms for each decay mode in which the events are weighted by the appropriate R

[**]The assumption is this final state is an incoherent superposition of vector resonances that should dominate this mode; here the nonresonant channel includes all the modes not explicitly considered such as $f_0K^-\pi^+\pi^+$.

[††]We have selected two of these submasses to correspond to those in which the resonances we are considering would peak if present. The $(\pi^+\pi^+)$ submass was included so that we could make the number of fitted bins exceed the number of fit parameters and thus avoid a zero constraint fit. Although a zero constraint is possible it leaves us with no χ^2 estimate of the goodness of fit.

matrix element[‡‡] and determine the acceptance corrected yield by fitting the distribution to a Gaussian function for the signal over a linear background. Using Monte Carlo simulated mixtures of these four decay modes we verified that biases in the corrected yields determined by this procedure are much smaller than the reported statistical errors and that the results are not sensitive to variations in reasonable choices for the resonance peak regions.

The final results (expressed as acceptance corrected yields) are summarized in Table III and the four weighted histograms with fits superimposed are shown in Fig.2. The 5^{th} histogram (Fig.2e), which is the sum of all the modes combined, is equivalent to the $K^-\pi^-\pi^+\pi^+\pi^+$ mass distribution (see Fig.1b) after correction for efficiency. The overall fit quality is evaluated by comparing the predicted signal yields in each of the submass bins with the observed signal yields, as shown in Fig.3. The calculated χ^2 is 2.75 (4 degrees of freedom) for a confidence level of 60%. We assessed the systematic errors on the resonant fraction of Table III, by gauging the stability of the results to 50% variations on the width of the submass bins centered about the ρ^0 and $\overline{K^{*0}}$.

We calculated the relative branching ratios by dividing the acceptance corrected yields of Table III by the corrected yield (201664 $\pm$ 1950) for the normalizing decay mode $D^+ \rightarrow K^-\pi^+\pi^+$; the systematic errors are derived from the systematic of the inclusive mode $K^-\pi^-\pi^+\pi^+\pi^+$(see Table I) and the systematics on the resonant fractions reported in Table III. Our results are summarized and compared to other recent measurements in Table IV. The disagreement between our result for the branching ratio $\Gamma(\overline{K^{*0}}\rho^0\pi^+)/\Gamma(\overline{K^{*0}}\pi^-\pi^+\pi^+)_{incl.}$ and the E691 measurement [1] may be due to the indirect way they used to calculate the amount of ρ^0: they cut around the $\overline{K^{*0}}$ mass and determined the content of ρ^0 from a fit to the highest remaining $\pi^-\pi^+$ mass combination.

In conclusion, we have measured the relative branching ratios of $D^+ \rightarrow K^-\pi^-\pi^+\pi^+\pi^+$,

---

‡‡The weight is the R matrix element having a row number corresponding to the decay mode and column number given by the submass bin.

$D_s^+ \to K^- K^+ \pi^- \pi^+ \pi^+$, $D_s^+ \to \phi \pi^- \pi^+ \pi^+$ and have presented the first compelling evidence of the decay mode $D^+, D_s^+ \to \pi^- \pi^- \pi^+ \pi^+ \pi^+$. Our analysis of the resonance substructure in the decay $D^+ \to K^- \pi^- \pi^+ \pi^+ \pi^+$ shows some differences with respect to the previous E691 measurements [1]. Our analysis support the interpretation that the nonresonant component in nonleptonic decays of the D^+ meson is small; the one exception to this pattern is the decay $D^+ \to K^- \pi^+ \pi^+$ which cannot be described without a large nonresonant component [10].

We wish to acknowledge the assistance of the staffs of the Fermi National Accelerator Laboratory, the INFN of Italy, and the physics departments of the collaborating institutions. This research was supported in part by the National Science Foundation, the U.S. Department of Energy, the Italian Istituto Nazionale di Fisica Nucleare and Ministero dell'Università e della Ricerca Scientifica e Tecnologica, and the Korean Science and Engineering Foundation.

REFERENCES

[a] Present address: Fermilab, Batavia, IL 60510, USA.

[b] Present address: University of Maryland, College Park, MD 20742, USA.

[c] Present address: University of South Carolina, Columbia, SC 29208, USA.

[d] Present address: Vanderbilt University, Nashville, TN 37235, USA.

[e] Present address: Enrico Fermi Institute, University of Chicago, Chicago, IL 60637, USA.

[f] Present address: Department of Physics, Indiana University, Bloomington, Indiana, IN 47405, USA.

[g] Present address: Syracuse University, Syracuse, NY 13244-1130, USA.

[h] Present address: University of Colorado, Boulder, CO 80309, USA.

[i] Present address: University of New York, Stony Brook, NY 11794, USA.

[j] Present address: AT&T, West Long Branch, NJ 07765, USA.

[k] Present address: Pohang Accelerator Laboratory, Pohang, Korea.

[l] Present address: Science Applications International Corporation, McLean, VA 22102, USA.

[m] Present address: Gamma Products Inc., Palos Hills, IL 60465, USA.

[n] Present address: Department of Physics and Astronomy, University of Pittsburgh, 3941 O'Hara St., Pittsburgh, PA 15260, USA.

[o] Present address: Brookhaven National Laboratory, Upton, NY 11793-5000, USA.

[p] Present address: KEK, National Laboratory for High Energy Physics, Tsukuba 305, Japan.

[1] E691 Collab., J.C.Anjos et al., Phys. Rev. D 42 (1990) 2414.

[2] E691 Collab., J.C.Anjos et al., Phys. Rev. Lett. 62 (1989) 125.

[3] ACCMOR Collab., S.Barlag et al., Z.Phys. C55 (1992) 383.

[4] M.Bauer, B.Stech, M.Wirbel, Z. Phys. C 34 (1987) 103;

P.Bedaque, A.Das and V.S.Mathur, Phys. Rev. D 49 (1994) 269;

B.Y.Block and M.A.Shifman, Sov. J. Nucl. Phys. 45 (1987) 522;

F.Buccella, M.Lusignoli, G.Miele, A.Pugliese, P.Santorelli Phys. Rev. D51 (1995) 3478;

L.L.Chau, H.Y.Cheng, Phys. Rev. D 36 (1987) 137;

M.Gibilisco, G.Preparata, Phys. Rev. D 47 (1993) 4949.

[5] T.E.Browder, K.Honscheid, D.Pedrini, Annu.Rev.Nucl.Part.Sci. 46 (1996) 395.

[6] E687 Collab., P.L.Frabetti et al., Phys. Lett. B 354 (1995) 486.

[7] E687 Collab., P.L.Frabetti et al., Nucl. Instrum. Methods A 320 (1992) 519.

[8] E687 Collab., P.L.Frabetti et al., Phys. Lett. B 351 (1995) 591.

[9] Particle Data Group, R.M.Barnett et al., Phys. Rev. D 54 (1996) 1.

[10] E687 Collab., P.L.Frabetti et al., Phys. Lett. B 331 (1994) 217.

[11] E687 Collab., P.L.Frabetti et al., Phys. Lett. B 281 (1992) 167.

[12] E691 Collab., J.C.Anjos et al., Phys. Rev. Lett. 60 (1988) 897.

[13] ARGUS Collab., H.Albrecht et al., Phys. Lett. B 153 (1985) 343.

TABLES

TABLE I. Branching ratios for $\Gamma(D^+ \rightarrow \text{Decay Mode})/\Gamma(D^+ \rightarrow K^-\pi^+\pi^+)$, $\Gamma(D_s^+ \rightarrow \text{Decay Mode})/\Gamma(D_s^+ \rightarrow K^-K^+\pi^+)$ and comparison to previous measurements.

Decay mode	E687 (This work)	E691
$D^+ \rightarrow \pi^-\pi^-\pi^+\pi^+\pi^+$	$0.023 \pm 0.004 \pm 0.002$	< 0.019 $(90\% C.L.)$ [2]
$D_s^+ \rightarrow \pi^-\pi^-\pi^+\pi^+\pi^+$	$0.158 \pm 0.042 \pm 0.031$	
$D^+ \rightarrow K^-\pi^-\pi^+\pi^+\pi^+$	$0.077 \pm 0.008 \pm 0.010$	$0.09 \pm 0.01 \pm 0.01$ [1]
$D_s^+ \rightarrow K^-K^+\pi^-\pi^+\pi^+$	$0.188 \pm 0.036 \pm 0.040$	

TABLE II. Branching ratio for $\Gamma(D_s^+ \rightarrow \phi\pi^-\pi^+\pi^+)/\Gamma(D_s^+ \rightarrow \phi\pi^+)$ and comparison to previous measurements.

Experiment	$\Gamma(D_s^+ \rightarrow \phi\pi^-\pi^+\pi^+)/\Gamma(D_s^+ \rightarrow \phi\pi^+)$
E687 (This work)	$0.28 \pm 0.06 \pm 0.01$
E687 (87-88) [11]	$0.58 \pm 0.21 \pm 0.10$
E691 [12]	$0.42 \pm 0.13 \pm 0.07$
ARGUS [13]	$1.11 \pm 0.37 \pm 0.28$

TABLE III. Yields corrected by efficiency and acceptance and fractions relative to the inclusive mode for the resonance substructure of the $D^+ \rightarrow K^-\pi^-\pi^+\pi^+\pi^+$ decay mode. These values have not been corrected for branching ratios into unobserved decay modes of the intermediate resonances.

Decay Mode	Corrected Yield	Fraction
$(K^-\pi^-\pi^+\pi^+\pi^+)_{NR}$	-1159 ± 2445	$0. \pm 0.16 \pm 0.01$
$\overline{K^{\star 0}}\pi^-\pi^+\pi^+$	6508 ± 2039	$0.42 \pm 0.14 \pm 0.08$
$K^-\rho^0\pi^+\pi^+$	6890 ± 1824	$0.44 \pm 0.13 \pm 0.04$
$\overline{K^{\star 0}}\rho^0\pi^+$	3148 ± 1300	$0.20 \pm 0.09 \pm 0.05$
Inclusive $K^-\pi^-\pi^+\pi^+\pi^+$	15550 ± 1542	1.

TABLE IV. Branching ratios measurements for the resonance substructure of the $D^+ \rightarrow K^-\pi^-\pi^+\pi^+\pi^+$ decay mode. We measured the first 4 branching ratios, the last two results are shown for a comparison with the previous measurements by E691. The branching ratios for the unseen decay modes of intermediate resonances have been included where appropriate.

Branching ratio	E687(this work)	E691 [1]
$\frac{\Gamma(K^-\pi^-\pi^+\pi^+\pi^+)_{NR}}{\Gamma(K^-\pi^+\pi^+)}$	$< 0.026 \quad (90\% C.L.)$	
$\frac{\Gamma(\overline{K^{*0}}\pi^-\pi^+\pi^+)}{\Gamma(K^-\pi^+\pi^+)}$	$0.048 \pm 0.015 \pm 0.011$	
$\frac{\Gamma(K^-\rho^0\pi^+\pi)}{\Gamma(K^-\pi^+\pi^+)}$	$0.034 \pm 0.009 \pm 0.005$	
$\frac{\Gamma(\overline{K^{*0}}\rho^0\pi^+)}{\Gamma(K^-\pi^+\pi^+)}$	$0.023 \pm 0.010 \pm 0.006$	
$\frac{\Gamma(\overline{K^{*0}}\pi^-\pi^+\pi^+)_{incl.}}{\Gamma(K^-\pi^-\pi^+\pi^+\pi^+)}$	$0.93 \pm 0.25 \pm 0.19$	$1.25 \pm 0.12 \pm 0.23$
$\frac{\Gamma(\overline{K^{*0}}\rho^0\pi^+)}{\Gamma(\overline{K^{*0}}\pi^-\pi^+\pi^+)_{incl.}}$	$0.33 \pm 0.11 \pm 0.08$	$0.75 \pm 0.17 \pm 0.19$

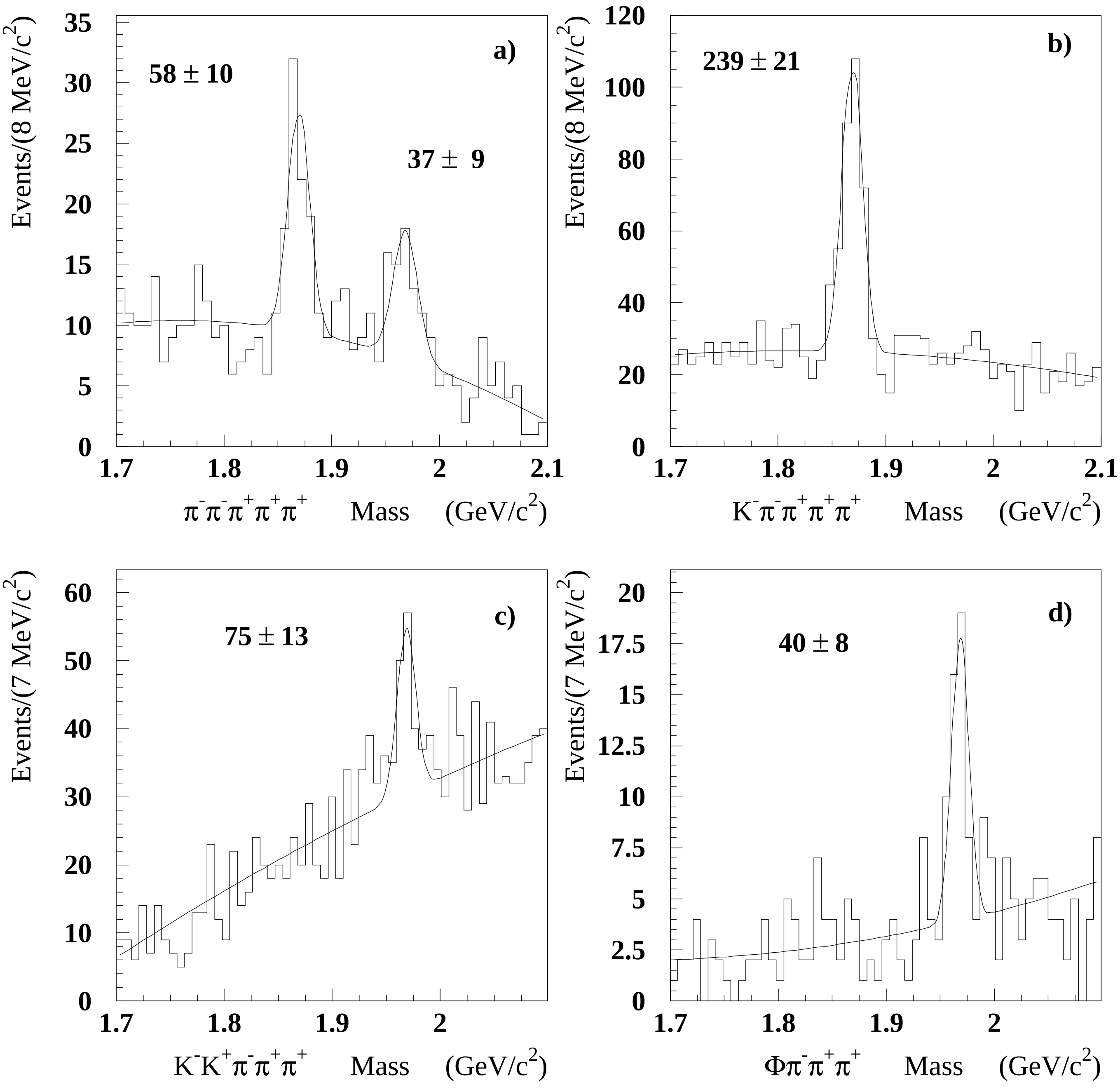

Fig. 1: (a) 5π invariant mass distribution. (b) $K4\pi$ invariant mass distribution. (c) $KK3\pi$ invariant mass distribution. (d) $\phi3\pi$ invariant mass distribution. The fits (solid curves) are described in the text and the numbers quoted are the yields.

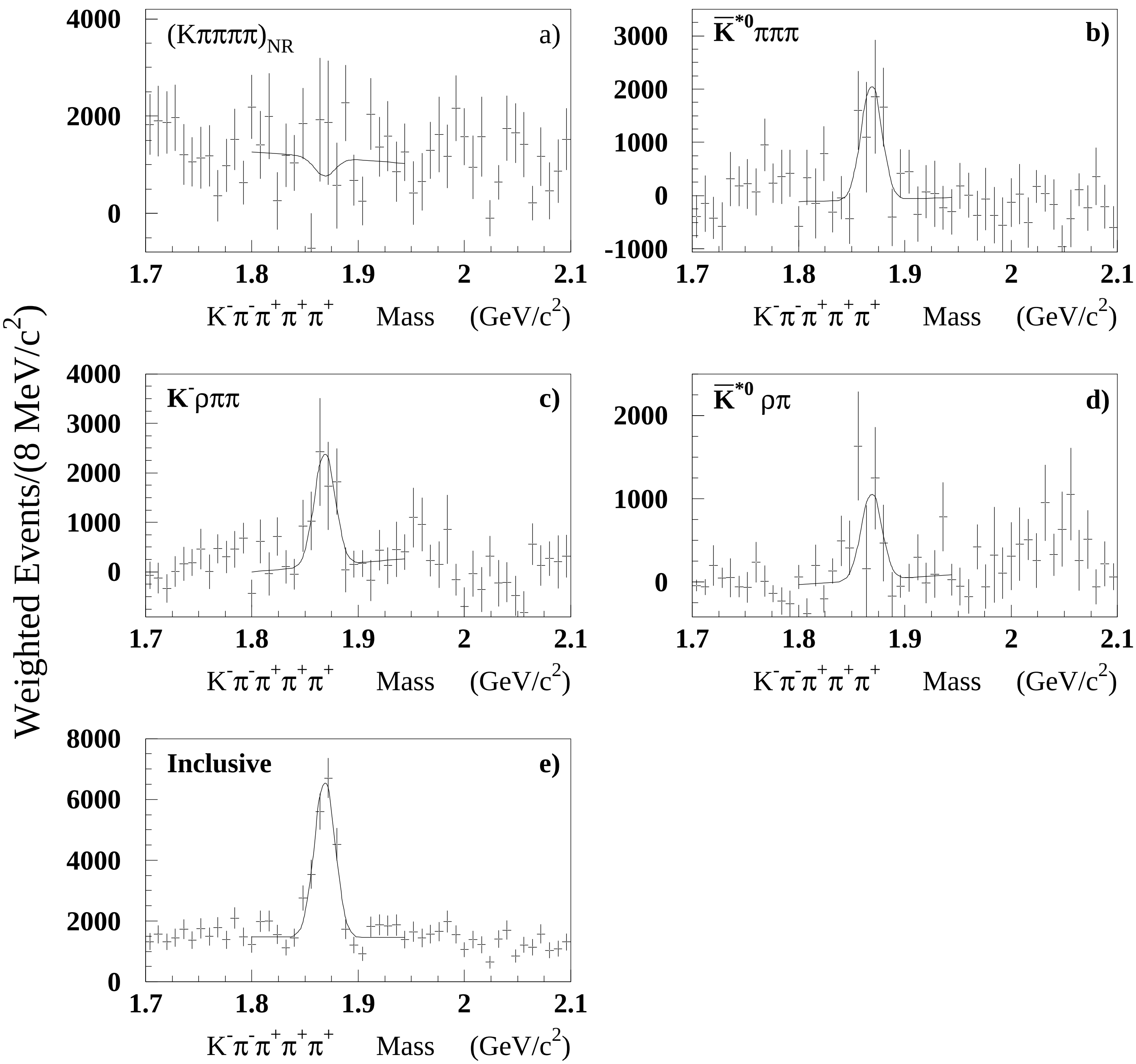

Fig. 2: $K^-\pi^-\pi^+\pi^+\pi^+$ weighted invariant mass for (a) $(K^+\pi^-\pi^+\pi^+\pi^+)_{NR}$ decay mode, (b) $\overline{K^{\star 0}}\pi^-\pi^+\pi^+$ decay mode, (c) $K^-\rho^0\pi^+\pi^+$ decay mode, (d) $\overline{K^{\star 0}}\rho^0\pi^+$ decay mode, (e) Inclusive : sum of all the 4 modes. The fits (solid curves) are to a Gaussian for the signal over a linear background.

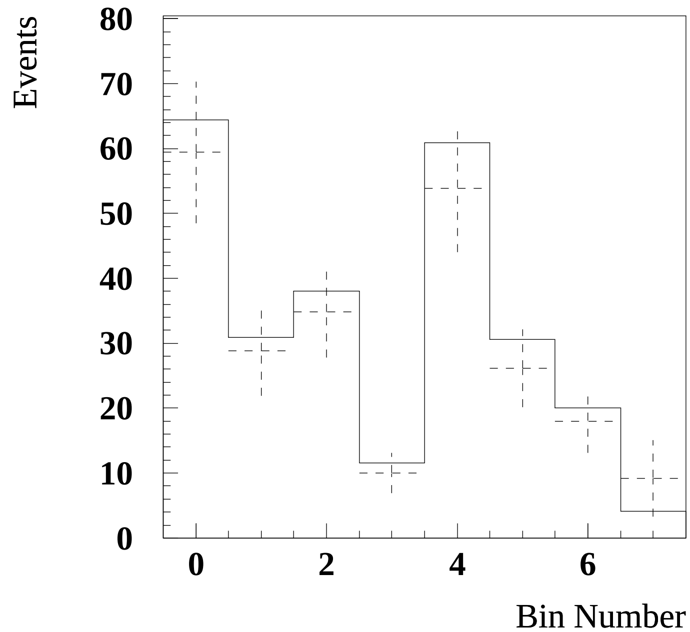

Fig. 3: The solid histogram is the signal yield predicted by the fit while the dashed points are the observed signal yields in each of the 8 submass bins, for the $K^-\pi^-\pi^+\pi^+\pi^+$ final state. The submass bins are defined by numbers η which have the value 1(0) if the submass is within(outside) a resonance peak region or greater(lower) than the mean for the submass $\pi^+\pi^+$, according to the mapping:

bin number $= 1\eta_{K^-\pi^+} + 2\eta_{\pi^-\pi^+} + 4\eta_{\pi^+\pi^+}$.